

Origin of electrophosphorescence from a doped polymer light emitting diode

P. A. Lane,^{1*} L. C. Palilis,¹ D. F. O'Brien,² C. Giebeler,¹ A. J. Cadby,^{1†} D. G. Lidzey,¹ A. J. Campbell,^{1†} W. Blau,² and D. D. C. Bradley^{1†}

¹*Department of Physics and Astronomy, University of Sheffield, Sheffield S3 7RH, United Kingdom*

²*Physics Department, Trinity College, Dublin, Ireland*

(Received 26 July 2000; revised manuscript received 2 November 2000; published 31 May 2001)

The origin of electrophosphorescence from a doped polymer light emitting diode (LED) has been investigated. A luminescent polymer host, poly(9,9-dioctylfluorene) (PFO), was doped with a red phosphorescent dye, 2,3,7,8,12,13,17,18-octaethyl-21H,23H-porphyrin platinum(II) (PtOEP). The maximum external quantum efficiency of 3.5% was obtained at a concentration of 4% PtOEP by weight. Energy transfer mechanisms between PFO and PtOEP were studied by absorption, photoluminescence, and photoinduced absorption spectroscopy. Even though electroluminescence spectra were dominated by PtOEP at a concentration of only 0.2 wt % PtOEP, Förster transfer of singlet excitons was weak and there was no evidence for Dexter transfer of triplet excitons. We conclude that the dominant emission mechanism in doped LED's is charge trapping followed by recombination on PtOEP molecules.

DOI: 10.1103/PhysRevB.63.235206

PACS number(s): 78.60.Fi, 34.30.+h, 72.20.Jv, 32.50.+d

I. INTRODUCTION

The performance of polymer light emitting diodes (LED's) has improved dramatically over the last decade. The brightness, lifetime, stability, and efficiency of these devices are rapidly approaching the levels needed for commercial application.^{1,2} Until recently the radiative mechanism in polymer LED's was fluorescence, the spin allowed ($\Delta S = 0$) dipole emission of light from singlet excited states. Exciton formation in polymer LED's follows the Coulomb capture of nongeminate pairs of oppositely charged polarons injected from the electrodes. Consequently both singlet ($S = 0$) and triplet ($S = 1$) excited states are formed with spin statistics predicting a 25% yield of singlet excitons. This calculation assumes similar cross sections for formation of triplets and singlets and has recently come under question. Singlet formation rates as high as 50% have been proposed.^{3,4} Radiative recombination of both singlet and triplet states substantially increases the theoretical electroluminescence efficiency of organic LED's.

Phosphorescent dyes have been used in organic LED's to overcome the efficiency limit imposed by formation of triplet excitons.⁵⁻¹⁶ These materials incorporate a heavy metal atom with strong spin-orbit coupling that mixes singlet and triplet states. Phosphorescence, the radiative recombination of triplet states, becomes allowed. The efficiency of intersystem crossing from the singlet to triplet excited states is also enhanced. As a result, the lowest triplet state is efficiently populated and can give light emission. For example, the phosphorescence efficiency of 2,3,7,8,12,13,17,18-octaethyl-21H,23H-porphyrin platinum(II) (PtOEP) is four orders of magnitude higher than its fluorescence efficiency.⁵ For these devices, the phosphorescent dopant is incorporated into a fluorescent host, either a small molecule host,⁵⁻¹¹ a polymer with a luminescent sidechain chromophore,^{12,13} or a π -conjugated polymer.¹³⁻¹⁵ Internal quantum efficiencies of 23% for PtOEP in dicarbazole biphenyl⁶ and 32% for tris(2-phenylpyridine) iridium in dicarbazole biphenyl⁸ have been reported. These high efficiencies demonstrate the potential

arising from the use of phosphorescent dopants as emissive centers in organic displays.

Both Förster and Dexter transfer can play a role in phosphorescent LED's. Förster transfer is a resonant dipole coupling process that transfers energy between singlet states and conserves the spin state of the donor and acceptor chromophores. It is dependent on the energetic overlap between the donor emission spectrum and the acceptor absorption spectrum and has an inverse sixth power dependence on the donor-acceptor separation.¹⁷ The efficacy of Förster transfer between two specific materials can be characterized by a Förster transfer radius R_0 . This corresponds to the average separation between donor and acceptor for which the probability of transfer is equal to the probability of recombination on the donor. Förster transfer radii as high as 5 nm have been reported.^{18,19} Dexter transfer requires quantum mechanical tunneling of electrons between the donor and acceptor. It is therefore a shorter range process requiring donor-acceptor separations of less than 1 nm. Unlike Förster transfer, Dexter transfer preserves the total spin of the system, but not the spin of the donor and acceptor. Dexter transfer thus allows triplet-triplet energy transfer from donor to acceptor. This can occur when there is spectral overlap between the phosphorescence emission spectrum of the host and the singlet ground state to first triplet excited state absorption spectrum of the guest. This ensures an energetic overlap of the states between which tunneling occurs.

We wish to investigate a π -conjugated polymer suitable for Dexter transfer to PtOEP. The phosphorescence peak of PtOEP is at 646 nm, requiring a polymer with a triplet state energy greater than 2 eV. A serious problem arises in using π -conjugated polymers as the host in phosphorescent LED's, because the singlet-triplet splitting is quite large. Recent measurements by Romanovskii *et al.* have shown that the zero phonon fluorescence and phosphorescence peaks of a ladder-type poly(*para*-phenylene) are separated by 0.62 eV.²⁰ This would suggest the use of a polymer with fluorescence peak below 480 nm (2.58 eV). We have accordingly chosen poly(9,9-dioctylfluorene) (PFO) as the host for phos-

phorescent LED's. The 0-0 fluorescence peak of PFO lies at 423 nm,²⁴ which would imply that the lowest triplet excited state is approximately 2.3 eV above the ground state.

Despite the technological importance of phosphorescent LED's, energy transfer in such systems has received relatively little attention. Baldo *et al.* showed that there was evidence for Dexter transfer by comparing doped and undoped LED's.⁵ A more direct approach is to compare triplet state dynamics of the host and the host-guest blend. PFO and PtOEP are an attractive combination for such a study as the triplet lifetimes in the two systems differ by more than an order of magnitude. Photoinduced absorption measurements have shown that the triplet lifetime in PFO is a few milliseconds,^{21,22} whereas the phosphorescence lifetime of PtOEP is 91 μ s in a polystyrene host.⁵ If significant Dexter transfer occurred from PFO to PtOEP, this would effectively open up a new, fast recombination channel. Hence, the PFO triplet lifetime should significantly decrease. Even if Dexter transfer were relatively inefficient, the much longer triplet lifetime of PFO would result in an extension in the PtOEP phosphorescence lifetime. This reasoning is borne out by a recent study of organic LED's in which the phosphorescent dye Ir(ppy)₃ was used to sensitize a fluorescent dye (DCM2).⁹ The radiative lifetime of DCM2 was extended to follow the decay rate of Ir(ppy)₃ triplets.

We describe the experimental techniques used in this work in Sec. II, studies of the operation of phosphorescent LED's in Sec. III, and spectroscopic studies of PtOEP/PFO blends in Sec. IV. Electroluminescence spectra of LED's made from PtOEP/PFO blends are dominated by PtOEP emission, even at PtOEP concentrations as low as 0.2% by weight. Absorption and photoluminescence spectra of PtOEP/PFO blends show that Förster transfer is weak, requiring high loading of PtOEP to quench PFO fluorescence. Measurements of triplet state dynamics in PFO by photoinduced absorption spectroscopy show that virtually no Dexter transfer occurs. We conclude that PtOEP molecules in LED's are electrically excited by direct charge trapping of holes on PtOEP followed by electron capture and recombination rather than by formation of excitons on the host followed by energy transfer to PtOEP. This conclusion is supported by the increase of the operating voltage with increasing PtOEP concentration. This electrophosphorescence mechanism permits the fabrication of efficient red LED's despite weak energy transfer coupling between PFO and PtOEP.

II. EXPERIMENTAL METHODS

PtOEP was purchased from Porphyrin Products Inc.²³ and used without further purification. PFO is a well-characterized material that has been used as both an emissive and a transport layer in polymer LED's (see Fig. 1).²⁴ The synthesis and characterization of PFO have been previously described;²⁵⁻²⁷ PFO has an ionization potential of 5.8 eV and an optical gap of 3.0 eV.²⁸ For optical measurements, samples of PFO and PtOEP/PFO blends were spin-coated onto synthetic quartz (Spectrosil B) disks from toluene solution. A solution containing the polymer at a concentration of 15 mg/ml was spun

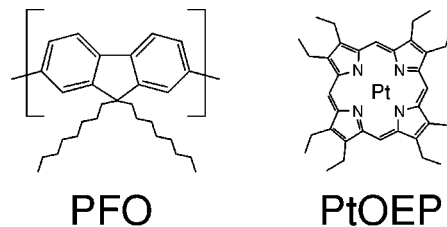


FIG. 1. The repeat unit of PFO and the chemical structure of PtOEP.

at a rate of 3500 rpm to give a film thickness of 150 nm. Film thicknesses were measured using a surface profilometer. To prepare the doped PFO films weighed amounts of PtOEP were added to produce solutions with concentrations up to 8% of PtOEP by weight. These were then spin-coated as for the pure PFO and gave the same film thickness.

Absorption spectra were measured in a Unicam UV-vis spectrophotometer. Photoluminescence (PL) emission was collected with an optical fiber, dispersed in a spectrograph, and recorded with an Oriel charge-coupled device (CCD) detector. For this measurement, samples were excited by a monochromated 150 W xenon arc lamp. Absorption and luminescence measurements were performed in an ambient environment at 300 K. The Förster transfer radius R_0 is defined as the donor-acceptor distance for which the probability of intermolecular energy transfer is equal to that of fluorescence. The Förster radius can be independently calculated by comparing the fluorescence spectrum of PFO with the absorption spectrum of PtOEP. The expected relation is

$$R_0^6 = \frac{0.5291K^2}{N_A n^4} \int \frac{F_m(E) \epsilon_Q(E) dE}{E^4}, \quad (1)$$

where K^2 is an orientation factor (2/3 for random orientation), N_A is Avogadro's number, n is the refractive index of the host, F_m is the normalized fluorescence spectrum of the host, ϵ_Q is the molar decadic extinction coefficient of the guest, and E is the energy in wave numbers.²⁹

The LED's studied were bilayer structures with an indium tin oxide (ITO) anode, a hole transport layer of *N,N*-di(3-hydroxycarbonyl-phenyl)-*N,N*-diphenylbenzidine (BFA), an electron transport and emissive layer of PFO/PtOEP, and a calcium cathode. All polymer solutions were passed through a 0.5 μ m pore filter before spin-coating. Devices with an active area of 4 mm² were fabricated and tested in a nitrogen atmosphere. BFA was spin-coated from a 10 mg/ml dimethylformamide solution at a speed of 3000 rpm, to give a 45 nm thick film. This layer was then baked at 60 °C for 300 min under rotary vacuum to remove residual solvent. The PFO and PtOEP/PFO doped layers were spin-coated from a 15 mg/ml toluene solution at a speed of 3500 rpm to give a thickness of 150 nm. BFA is not soluble in toluene and so the second layer can be deposited without dissolving the first layer. A calcium cathode was evaporated onto the emissive layer to give the final device structure ITO:BFA:PFO/PtOEP:Ca. LED's containing PtOEP doping concentrations of 0.2% to 8% by weight were investigated.

Pulsed driving of the LED's was also examined. The bias voltage pulses had a magnitude of 70 V, a 4 μ s duration,

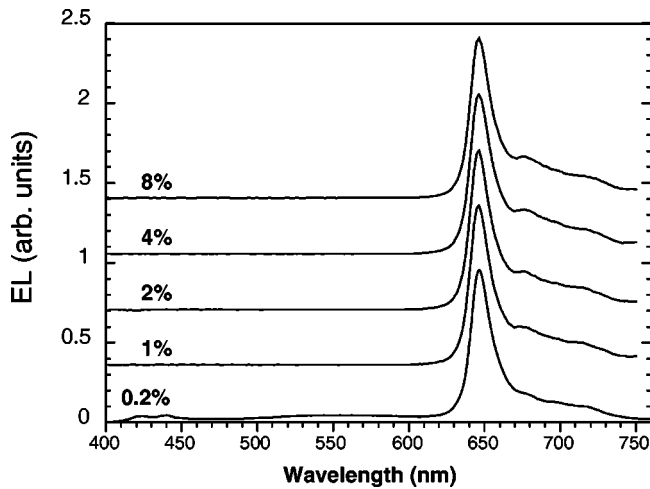


FIG. 2. The electroluminescence spectra of PtOEP/PFO LED's. The spectra are normalized to the phosphorescence peak at 646 nm and offset for comparison.

and were spaced at 1 ms intervals. The pulsed electroluminescence (EL) measurements were carried out under a vacuum of 10^{-6} mbar. Luminance values were measured using a Topcon BM8 luminance meter. The external electroluminescence quantum efficiency η_{EL} was determined by collecting light emitted in the forward direction only.

Photoinduced absorption (PA) spectroscopy was employed to compare triplet state dynamics in PFO films and PtOEP/PFO blends. PA spectroscopy uses standard phase-sensitive lock-in techniques with a modulated pump beam to excite the material and a broad spectrum light source as a probe. Films for PA measurements were prepared as for PL and absorption. The PA spectrum, defined as the normalized change ΔT in the probe transmission T , is proportional to the photoexcitation density, the excitation cross section, and the sample thickness. The excitation lifetime can be determined by measuring the dependence of the PA upon the modulation frequency. For monomolecular recombination kinetics, the magnitude of the PA signal depends upon the modulation frequency as

$$\Delta T \propto [1 + (\omega\tau)^2]^{-0.5}, \quad (2)$$

where T is the transmission through the sample, ω is the pump modulation frequency (in rad/s), and τ is the excitation lifetime.^{30,31} This relationship was also used to determine the phosphorescence lifetime of PtOEP.

III. STUDIES OF PHOSPHORESCENT LIGHT EMITTING DIODES

Figure 2 shows the EL spectra of LED's with concentrations between 0.2% and 8% PtOEP by weight, measured at a current density $J=22$ mA/cm². The spectra are normalized to the EL peak at $\lambda=646$ nm and offset for ease of comparison. All devices have an EL spectrum characteristic of PtOEP emission, with a peak at 646 nm and vibronic sidebands at 685 nm and 718 nm. The 0.2 wt % doped device also shows a weak peak at $\lambda=430$ nm characteristic of

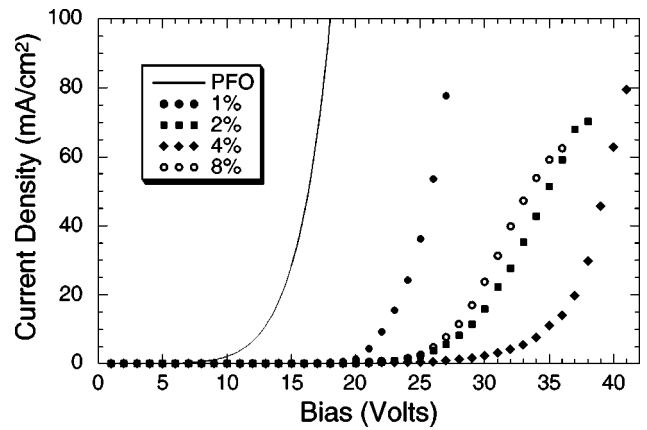


FIG. 3. The current density as a function of applied bias of a PFO LED and PtOEP/PFO LED's with PtOEP concentrations of 1%, 2%, 4%, and 8% by weight.

PFO fluorescence and a broad emission band peaked at 550 nm which has previously been assigned to excimer emission in PFO.³² No PFO emission was detected from the other devices and no fluorescence was detected from the PtOEP singlet at $\lambda=580$ nm for any device.³³

Figures 3 and 4 show the dependence of the current density and luminance, respectively, on the applied bias for doping concentrations of 1%, 2%, 4%, and 8% by weight. Measurements of an undoped PFO LED are shown for comparison; the structure of the PFO LED was ITO/(60 nm BFA)/(200 nm PFO)/Ca.²⁴ The operating voltage required for charge injection and the onset of electroluminescence increases with doping up to 4 wt % and then decreases for the 8 wt % sample. Table I shows the bias required for a current density of 5 mA/cm² and for a luminance of 5 cd/m². The operating voltage increases with increasing concentration, although there is a slight decrease in the bias required for 5 mA/cm² at 8 wt % doping. Tessler *et al.* have noted that the difference in the ionization potentials of PFO and PtOEP is greater than 0.5 V, making PtOEP a recombination center at concentrations as low as 0.01%.¹³ The increase of the

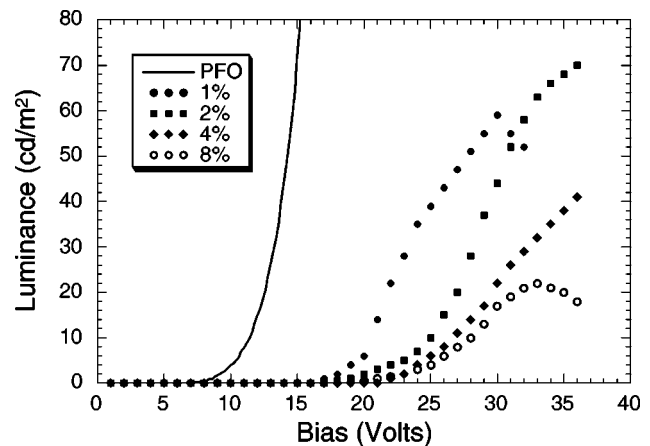


FIG. 4. The luminance as a function of applied bias of a PFO LED and of PtOEP/PFO LED's with PtOEP concentrations of 1%, 2%, 4%, and 8% by weight.

TABLE I. Summary of operating conditions of LED's prepared from blends of PFO and PtOEP.

PtOEP concentration (wt %)	Bias at 5 mA/cm ² (V)	Bias at 5 cd/m ² (V)	η_{EL}	Power efficiency (lm/W)	EL lifetime (μ s)
PFO only ^a	11.6	10.4 V	0.2%	0.069	not available
1	21	19.5	1.5%	0.096	
2	27	23	3%	0.177	56 \pm 5
4	33	24.5	3.5%	0.163	52 \pm 3
8	26	25.5	0.6%	0.03	54 \pm 3

^aReference 24.

operating voltage of doped LED's with increasing PtOEP concentration is clear evidence for charge trapping in the doped system.

It is possible to reduce the operating voltage of the doped LED's with PtOEP concentrations of 2 wt % and 4 wt % below 8 V by optimizing the thickness of individual layers and incorporating a hole injection layer of poly(3,4-ethylenedioxythiophene)/poly(styrenesulfonate).³⁴ The 4 wt % LED required a thinner active layer than the 2 wt % LED for optimum performance. Such work will not be discussed here, where our primary interest is an investigation of the physics of an identically prepared series of doped LED's rather than optimization of the performance of such devices.

The external quantum efficiency of phosphorescent LED's (η_{EL}) was deduced from the luminance and current data as previously reported.¹⁹ Figure 5 shows the variation of η_{EL} for the different PtOEP doping concentrations as a function of the LED luminance. The maximum η_{EL} values and power efficiencies are shown in Table I. In each case the efficiency peaks at a luminance below 10 cd/m². The maximum power efficiency for all devices was reached at a brightness below 10 cd/m². The efficiency drop at higher luminance is consistent with the behavior previously observed for doped small molecule devices.⁵

The maximum external EL efficiency of 3.5% is more than eight times that of optimized undoped PFO devices²⁴ and is nearly an order of magnitude greater than the previ-

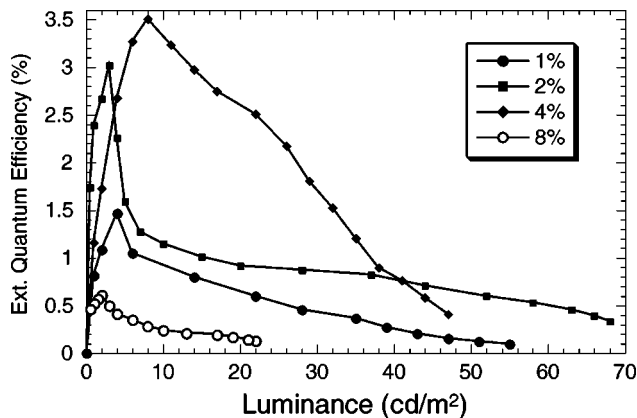


FIG. 5. The external quantum efficiency versus luminance of PtOEP/PFO LED's with PtOEP concentrations of 1%, 2%, 4%, and 8% by weight.

ously reported phosphorescent dopant/polymer host system of PtOEP doped PNP.¹² Guo *et al.* have recently reported an external quantum efficiency of 2.3% at a luminance of 11 cd/m² with a bilayer PFO device.¹⁵ The maximum efficiency in PtOEP doped PNP was observed at a significantly lower doping concentration (0.5%) than for PFO, perhaps due to the presence of different mechanisms for triplet formation on PtOEP (see below). A maximum luminance of \approx 200 cd/m² was observed here at a current density of 70 mA/cm² under dc operation. This gives an efficiency of 0.28 cd/A, very similar to that previously reported for an equally bright blue LED made with an ITO/BFA/PFO/Al structure with optimized layer thicknesses. When operated under pulsed driving, a peak brightness of 2000 cd/m² was observed for the LED containing 4 wt % PtOEP.

Figure 6 shows the decay of the EL of doped LED's under pulsed operation for concentrations of 0.2, 1, 4, and 8 wt % PtOEP in PFO. The data are arbitrarily scaled so as to be offset from one another. The EL decay could be fitted to a single exponential decay with a lifetime that did not vary significantly with PtOEP concentration. The EL lifetime of all devices was measured to be between 51 and 56 μ s and did not vary significantly with dopant concentration. These values are slightly lower than previously reported lifetimes of PtOEP in carbazole biphenyl (70 μ s),⁶ though higher than for aluminum tris quinolate.⁵ The single exponential

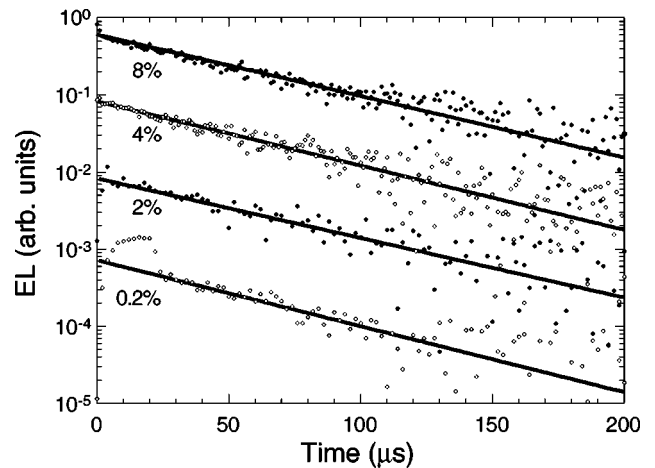


FIG. 6. The electrophosphorescence decay of doped PtOEP/PFO LED's at concentrations of 0.2%, 2%, 4%, and 8% by weight under pulsed operation. The bias voltage pulses had a magnitude of 70 V, a 4 μ s duration, and were spaced at 1 ms intervals.

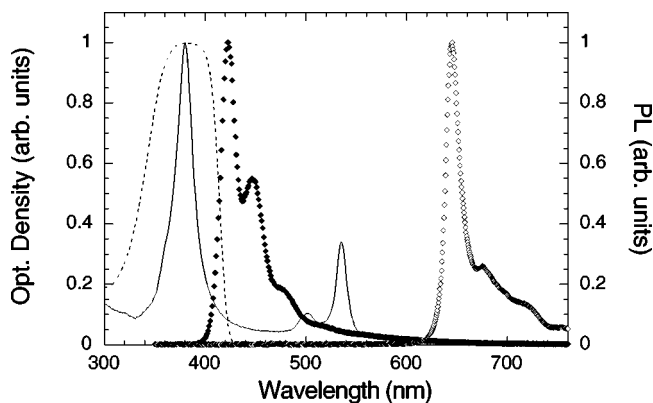


FIG. 7. The absorption spectra of PFO (dashed line) and PtOEP (solid line), the fluorescence spectrum of PFO (filled symbols), and the phosphorescence spectrum of PtOEP (open symbols).

decay is inconsistent with Dexter transfer occurring in our system. Dexter transfer typically takes place on a microsecond time scale;^{35,36} Cleave *et al.* recently reported a 10 ms time constant for Dexter transfer from PNP to PtOEP.¹² Dexter transfer would therefore be expected to lead to a signal with a rise time corresponding to the Dexter transfer rate and biexponential decay as observed by Harriman *et al.*³⁷ Investigations of Dexter transfer by photoinduced absorption spectroscopy are described in Sec. IV.

IV. SPECTROSCOPIC STUDIES OF BLENDS OF PTOEP AND PFO

There are three possible mechanisms for electrically exciting PtOEP molecules in the doped LED: (i) Förster transfer of PFO singlet excitons; (ii) Dexter transfer of PFO triplet excitons; and (iii) charge trapping followed by recombination on PtOEP molecules. The increase of the operating voltage (Figs. 3 and 4) upon doping is consistent with charge trapping, but does not rule out energy transfer nor can it determine which is the dominant excitation mechanism of PtOEP molecules. We have therefore undertaken spectroscopic studies in order to elucidate the underlying mechanism for electrophosphorescence. Förster transfer was studied by measuring the fluorescence spectrum of PFO and the absorption spectrum of PtOEP as well as the photoluminescence spectrum of blends as a function of PtOEP concentration. Dexter transfer was studied by using photoinduced absorption spectroscopy to compare triplet state dynamics of a PFO film and a PtOEP/PFO blend.

Figure 7 shows the absorption and fluorescence spectra of a PFO film and the absorption and phosphorescence spectra of PtOEP in PMMA at a concentration of 0.1% by weight. There is weak overlap between the fluorescence spectrum of PFO and the absorption spectrum of PtOEP. The Förster radius for PtOEP in PFO was calculated using Eq. (1) to be 1.7 nm; this will require relatively high doping concentrations to transfer singlet excitons from PFO to PtOEP. Such high concentrations would be required for effective Dexter transfer in any event. The excimer emission band at 550 nm has a relatively stronger contribution to the EL spectrum than to the

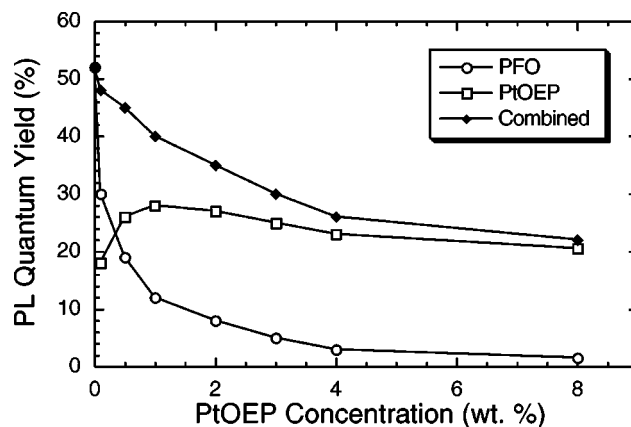


FIG. 8. The PFO fluorescence, PtOEP phosphorescence, and total photoluminescence efficiencies as a function of PtOEP concentration. The excitation source was the 354 nm line of a HeCd laser.

PL spectrum, although its relative strength varied among devices and depended upon the current density through the device. This feature is currently under investigation.

Figure 8 shows the fluorescence quantum yield of PFO, the phosphorescence quantum yield of PtOEP, and the total PL yield as a function of PtOEP concentration between 0 and 8% by weight. The samples were excited by a HeCd laser at 354 nm, where PtOEP absorption is quite weak. Virtually all of the absorption will be by the PFO host. The PL spectra of the PtOEP/PFO blends (not shown) are superpositions of the individual spectra of PFO and PtOEP (Fig. 7). The contribution of the PFO emission to the PL spectrum decreases significantly as the PtOEP dopant concentration increases. However, even at 8 wt% PtOEP concentration, emission from PFO is not completely quenched. The ratio of the PL yields of the blend components could be used to independently calculate the Förster transfer radius. Energy transfer is equally probable at a typical PtOEP separation of 1.9 nm (assuming a uniform dispersion of PtOEP in PFO). This value is in good agreement with the overlap integral calculation. The PtOEP phosphorescence quantum yield decreases from 28% at 1 wt% PtOEP to 20% at 8 wt% PtOEP.

There is some evidence for aggregation in the absorption spectra of PtOEP in a polystyrene host. We observed increased scattering and some splitting of the absorption spectrum at PtOEP concentrations above 0.2 wt%. We suggest that intermolecular interactions between PtOEP molecules are reducing the phosphorescence quantum yield. This is consistent with the lower applied bias required for a current density of 5 mA/cm² at 8 wt% PtOEP than at 2 or 4 wt% PtOEP. It is possible that the percolation threshold for conduction through PtOEP has been reached at a concentration of 8% by weight. This results in increased current, but not luminance, as holes conduct through the PtOEP and exit the device rather than being trapped.

A much higher PtOEP concentration is required to quench PFO emission for optical excitation than for electrical excitation. Consider the ratio of the emission peaks of PFO at 440 nm and PtOEP at 646 nm; the same calibrated CCD

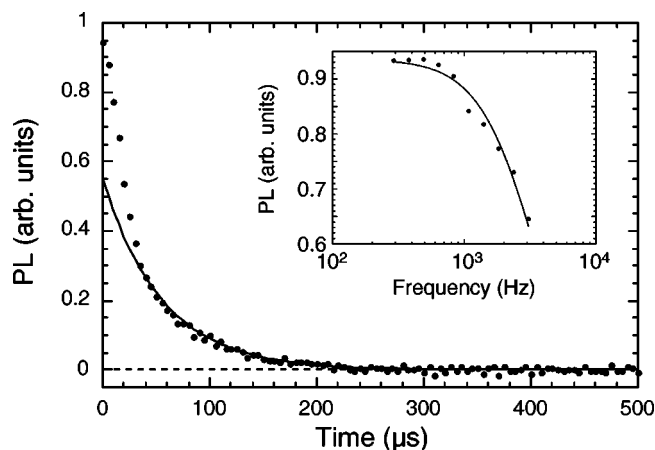


FIG. 9. Phosphorescence decay of a PtOEP/PFO blend following excitation. The symbols show experimental results and the solid line a fit to exponential decay. Inset: Dependence of the phosphorescence intensity of PtOEP, measured with a lock-in amplifier, on the pump modulation frequency. The symbols show the experimental results and the solid line is a fit to Eq. (2).

and spectrograph was used for both measurements. The ratio of these peaks in the EL spectra at 0.2 wt % doping (23.0) is nearly the same as that in the PL spectra at 8 wt % doping (23.3). Only 1 wt % of PtOEP is required to completely quench PFO emission in the electroluminescence spectra. Thus, Förster transfer of singlet excitons from PFO to PtOEP cannot account for dominant PtOEP emission at low dopant concentrations in the EL spectra shown in Fig. 2. Rather, a mechanism other than Förster transfer must be operating. In order to fully understand the physics of phosphorescent LED's, it is necessary to investigate Dexter transfer also. To determine whether Dexter transfer is also occurring, PFO triplet dynamics must be measured in PtOEP/PFO blends and compared to an undoped film of PFO.

The PtOEP triplet lifetime in a PFO matrix was determined by measuring the phosphorescence decay following photoexcitation. The phosphorescence decay of a blend containing 1 wt % PtOEP in PFO is shown in Fig. 9. The decay could be fitted to a lifetime of $55.3 \pm 1.5 \mu\text{s}$ (solid line), in excellent agreement with the pulsed EL measurements shown in Fig. 6. The deviation of the first 30 μs of the data from exponential decay is due to fluorescence from PFO and the fact that a blade chopper does not produce a pure square wave modulation. The phosphorescence lifetime was independently determined by measuring the dependence of the phosphorescence intensity on the laser modulation frequency and fitting the resulting data to Eq. (2). The result of this measurement is shown in the inset of Fig. 9. The symbols show the experimental results and the solid line a fit to the phosphorescence lifetime using Eq. (2). The phosphorescence lifetime was determined to be $56 \pm 3 \mu\text{s}$, in good agreement with the transient EL decay shown in Fig. 6 and the transient PL shown in Fig. 9.

Figure 10(a) shows the PA spectrum of an undoped PFO film, measured at 80 K. The PFO film was excited with a pump beam at $\lambda = 363 \text{ nm}$ modulated at a frequency of 200

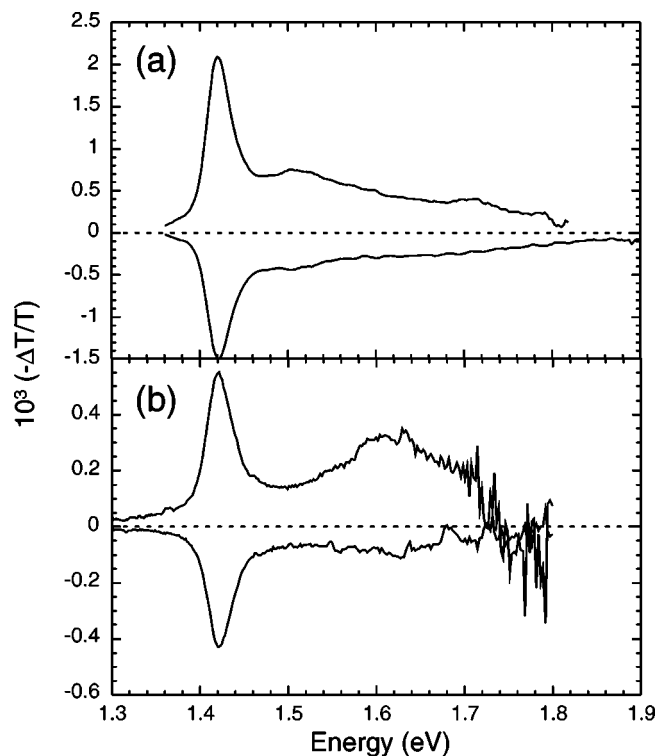


FIG. 10. In-phase (top) and quadrature (bottom) PA spectra of (a) an undoped film of PFO and (b) a blend containing 8 wt % PtOEP.

Hz with an optical blade chopper. The PA spectrum is dominated by a sharp transition at 1.43 eV with a weak vibronic sideband at 1.62 eV and PA extending up to 2 eV. PA-detected magnetic resonance measurements of PFO determined the transitions for charged polarons to be 0.4 eV and 1.93 eV.²¹ We accordingly assign the sharp peak to excited state absorption of triplet excitons. Such an assignment is also consistent with studies of ladder-type poly(*para*-phenylene) (LPPP), which has the same conjugated backbone as polyfluorene.^{38,39} In this system, the triplet excited state absorption is a sharp band at 1.3 eV. The PA spectrum of a doped PFO film containing 8 wt % PtOEP is shown in Fig. 10(b). The PFO triplet peak at 1.43 eV is the strongest feature in the PA spectrum of the blend, although there is an additional PA band between 1.5 and 1.7 eV. This additional PA band is correlated with the phosphorescence, having the same relative weight for the in-phase and quadrature components. The PA spectrum of a film containing 1 wt % PtOEP in PMMA (not shown) contains a PA band between 1.3 and 1.7 eV. We therefore assign the additional PA band in a PtOEP/PFO blend to excited state absorption by PtOEP triplets.

The spectrally narrow triplet PA band at 1.43 eV makes it possible to compare PFO triplet state dynamics in the doped and undoped systems in order to look for evidence of Dexter transfer. The lifetime of the excited triplet state of PFO was determined by measuring the dependence of the triplet PA signal upon the modulation frequency and modeling the resulting data by Eq. (2). A series of PA spectra of a PFO film

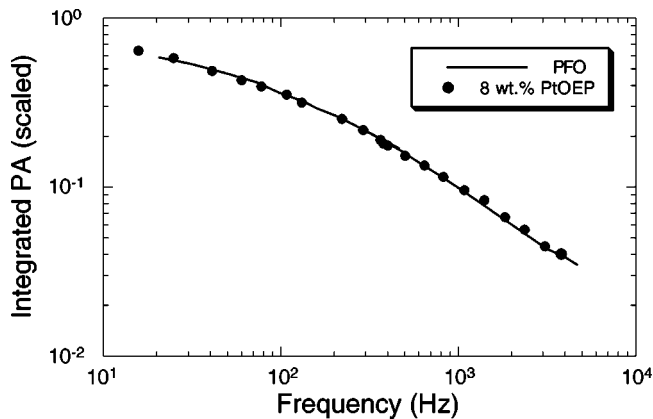


FIG. 11. The dependence of the triplet PA of PFO at 1.43 eV upon the pump modulation frequency for an undoped PFO film (symbols) and one containing 8 wt% PtOEP (solid line). The doped sample is scaled to the undoped sample for comparison.

and an 8 wt% PtOEP/PFO blend were measured as a function of the laser modulation frequency between 10 Hz and 4 kHz. The in-phase and quadrature PA spectra were integrated over the PFO triplet PA peak between 1.39 and 1.48 eV and the integrated root mean square PA signal was calculated. Figure 11 shows the frequency dependence of PFO triplet PA in a neat film of PFO as a solid line. The resulting data for PFO could not be fitted to a single excitation lifetime, but could be simulated by a bimodal lifetime distribution with lifetimes of 3.2 and 0.3 ms. The longer lifetime has 72% weighting and the shorter lifetime 28%.

The lifetime of PFO triplet excitons is much longer than the phosphorescence lifetime of PtOEP in PFO (Fig. 6). Dexter transfer from PFO to PtOEP should reduce the PFO triplet lifetime, because PtOEP molecules decay at a much more rapid rate (56 μ s) than PFO triplets (0.3 to 3.2 ms). The symbols in Figure 11 show the frequency dependence of the PFO triplet PA signal in an 8 wt% doped PFO film, measured under identical conditions as for the undoped film. There is no difference in the frequency dependences of the PA of the two different samples. Thus, if there is any Dexter transfer from PFO to PtOEP, it must be exceedingly weak. This conclusion is supported by the fact that there was no evidence for phosphorescence originating from Dexter transfer of relatively long lived PFO triplets. This is a rather surprising result as PFO should be a good candidate for Dexter transfer of triplets to PtOEP. We speculate that the orientation of PtOEP molecules in PFO is such that there is not a sufficient overlap of wave functions for Dexter transfer to occur.

V. CONCLUSIONS

Neither Förster nor Dexter transfer can account for changes in the EL spectra upon lightly doping (0.2 wt%) a PFO LED with PtOEP. We therefore propose that PtOEP molecules act as both hole traps and recombination centers. ITO:PFO:Ca devices are injection limited and the current is dominated by holes that have a high mobility.⁴⁰ The trapped

charges can subsequently recombine with electrons to generate both singlet and triplet states on the PtOEP. The singlets are converted to triplets via efficient intersystem crossing and thus also result in phosphorescence. Any singlet states formed directly on PFO by recombination of untrapped charges can subsequently Förster transfer to the PtOEP singlet and also contribute to the phosphorescence emission. As we find no evidence for Dexter transfer, we conclude that all excitons except PFO triplets are available to produce emission.

The increase of the operating voltage of the doped devices with increasing PtOEP concentration is a consequence of charge trapping on PtOEP molecules and reflects the dominance of hole injection and transport. Time-of-flight studies have shown that PFO is a trap-free transporter of holes.⁴⁰ The ionization potential of PtOEP is 0.5 eV less than that of PFO; therefore PtOEP will act to trap holes.¹² Charge trapping reduces the mobility of holes and thus much higher fields are required to transport significant amounts of charge through the device.

The EL quantum yield increases with increasing dopant concentration, reaching a maximum of 3.0% at 2 wt% doping and 3.5% at 4 wt% doping. We attribute these high efficiencies to better charge balance between positive and negative carriers in the recombination zone and the use of both singlet and triplet excited states to generate EL. The operating voltage and EL quantum efficiency decreased at PtOEP concentrations above 4% by weight. Interactions between PtOEP molecules at a concentration of 8% by weight are sufficiently strong that triplet quenching is seen in PL measurements. Films of PtOEP in PMMA show that intermolecular interactions are sufficient to change the absorption spectrum (Davidov splitting); the phosphorescence quantum yield is also reduced at this concentration. Measurements on PFO films doped by the red dye tetraphenyl porphyrin show similar results.¹⁹ It is plausible that charge transport occurs between the dopant molecules at such high concentrations. This would then increase hole mobilities through the device and reduce the trapped space charge and the EL efficiency.

In summary, we have fabricated LEDs using PtOEP doped PFO as the emissive layer. This notably improved the external quantum efficiency of electroluminescence when compared to undoped PFO devices. A maximum efficiency of 3.5% was obtained for a LED containing 4% PtOEP by weight in PFO. Weak Förster transfer of singlets was observed, but no Dexter transfer of triplets from the host to the dopant occurred. We propose that the increase in device efficiency is due to PtOEP acting as both a hole trap and a recombination center, enabling the use of both singlet and triplet excitons in the recombination process. This suggests that, even without a good overlap of the phosphorescence spectrum of the host with the singlet-triplet absorption spectrum of the dopant, phosphorescent dopants may be useful as a means to improve device efficiency.

ACKNOWLEDGMENTS

The authors would like to thank Mike Inbasekaran and Mark Bernius of the Dow Chemical Company for providing

the samples of PFO, Rob Fletcher for assistance with device preparation, and Alan Grice for measurements of undoped PFO LED's. The collaboration between Sheffield and Dublin was funded by a grant from the COST program of the European Commission and under the Esprit LTR project LUPO

(Project No. 28580). Research performed at the University of Sheffield was supported in part by the U.K. Engineering and Physical Sciences Research Council (Grants No. GR/L80775 and No. GR/M45115) and the Royal Society (Grant No. RS19025).

*Present address: C. S. Draper Laboratory, 555 Technology Square, Cambridge, MA 02139.

†Present address: Blakett Laboratory, Imperial College, Prince Consort Road, London SW7 2BW, United Kingdom.

- ¹K. Ziemelis, *Nature* (London) **399**, 408 (1999).
²*Proceedings of the Second International Conference on Electroluminescence of Molecular Materials and Related Phenomena*, edited by D.D.C. Bradley and P.A. Lane [Synth. Met. (to be published)].
³Y. Cao, I.D. Parker, G. Yu, C. Zhang, and A.J. Heeger, *Nature* (London) **397**, 414 (1999).
⁴Z. Shuai, D. Beljonne, R.J. Silbey, and J.L. Bredas, *Phys. Rev. Lett.* **84**, 131 (2000).
⁵M.A. Baldo, D.F. O'Brien, Y. You, A. Shoustikov, S. Sibley, M.E. Thompson, and S.R. Forrest, *Nature* (London) **395**, 151 (1998).
⁶D.F. O'Brien, M.A. Baldo, M.E. Thompson, and S.R. Forrest, *Appl. Phys. Lett.* **74**, 442 (1999).
⁷R.C. Kwong, S. Sibley, T. Dubovoy, M. Baldo, S.R. Forrest, and M.E. Thompson, *Chem. Mater.* **11**, 3709 (1999).
⁸M.A. Baldo, S. Lamansky, P.E. Burrows, M.E. Thompson, and S.R. Forrest, *Appl. Phys. Lett.* **75**, 4 (1999).
⁹M.A. Baldo, M.E. Thompson, and S.R. Forrest, *Nature* (London) **403**, 750 (2000).
¹⁰Y.G. Ma, C.M. Che, X.M. Zhou, W.H. Chan, and J.C. Shen, *Adv. Mater.* **11**, 652 (1999).
¹¹Y.G. Ma, T.S. Lai, and Y. Wu, *Adv. Mater.* **12**, 433 (2000).
¹²V. Cleave, G. Yahioglu, P. LeBarny, R.H. Friend, and N. Tessler, *Adv. Mater.* **11**, 285 (1999).
¹³N. Tessler, P.K.H. Ho, V. Cleave, D.J. Pinner, R.H. Friend, G. Yahioglu, P. Le Barny, J. Gray, M. de Souza, and G. Rumbles, *Thin Solid Films* **363**, 64 (2000).
¹⁴D.F. O'Brien, C. Giebeler, R.B. Fletcher, A.J. Cadby, L.C. Palilis, D.G. Lidzey, P.A. Lane, D.D.C. Bradley, and W. Blau, *Synth. Met.* **116**, 379 (2001).
¹⁵T.-F. Guo, S.-C. Chang, Y. Yang, R.C. Kwong, and M.E. Thompson, *Org. Electron.* **1**, 15 (2000).
¹⁶T. Förster, *Ann. Phys. (Leipzig)* **2**, 55 (1948).
¹⁷D.L. Dexter, *J. Chem. Phys.* **21**, 836 (1953).
¹⁸R.C.A. Keller, J.R. Silvius, and B. Dekruiff, *Biochem. Biophys. Res. Commun.* **207**, 508 (1995).
¹⁹T. Virgili, D.G. Lidzey, and D.D.C. Bradley, *Adv. Mater.* **12**, 58 (2000).

- ²⁰Y.V. Romanovskii, A. Gerhard, B. Schweitzer, U. Scherf, R.I. Personov, and H. Bassler, *Phys. Rev. Lett.* **84**, 1027 (2000).
²¹A.J. Cadby, P.A. Lane, S.J. Martin, D.D.C. Bradley, M. Wohlgenannt, C. An, and Z.V. Vardeny, *Synth. Met.* **111-112**, 515 (2000).
²²A.J. Cadby, P.A. Lane, H. Mellor, S.J. Martin, M. Grell, C. Giebeler, D.D.C. Bradley, M. Wohlgenannt, C. An, and Z.V. Vardeny, *Phys. Rev. B* **62**, 15 604 (2000).
²³Porphyryn Products Inc., P.O. Box 31, Logan, UT 84323-0031.
²⁴A.W. Grice, D.D.C. Bradley, M.T. Bernius, M. Inbasekaran, W.W. Wu, and E.P. Woo, *Appl. Phys. Lett.* **73**, 629 (1998).
²⁵N. Miyaura and A. Suzuki, *Chem. Rev.* **95**, 2457 (1995).
²⁶M. Bernius, M. Inbasekaran, E. Woo, W.S. Wu, and L. Wujkowski, *Proc. SPIE* **3621**, 93 (1999).
²⁷M. Grell, D.D.C. Bradley, X. Long, T. Chamberlain, M. Inbasekaran, E.P. Woo, and M. Soliman, *Acta Polym.* **47**, 439 (1998).
²⁸S. Janietz, D.D.C. Bradley, M. Grell, C. Giebeler, M. Inbasekaran, and E.P. Woo, *Appl. Phys. Lett.* **73**, 2453 (1998).
²⁹A. Shoustikov, Y. You, P. Burrows, M.E. Thompson, and S.R. Forrest, *Synth. Met.* **217**, 1 (1997).
³⁰C. Botta, S. Luzzati, R. Tubino, D.D.C. Bradley, and R.H. Friend, *Phys. Rev. B* **48**, 14 809 (1993).
³¹S.M.R. Rivkin, *Photoelectric Effects in Semiconductors* (Consultants Bureau, New York, 1964).
³²J. Teetsov and M.A. Fox, *J. Mater. Chem.* **9**, 2117 (1999).
³³G. Ponterini, N. Serpone, M. Bergkamp, and T.L. Netzel, *J. Am. Chem. Soc.* **105**, 4639 (1983).
³⁴L. Palilis, P.A. Lane, D.G. Lidzey, and D.D.C. Bradley (unpublished).
³⁵A.M. Brun and A. Harriman, *J. Am. Chem. Soc.* **116**, 10 383 (1994).
³⁶J. Sessler, B. Wang, and A. Harriman, *J. Am. Chem. Soc.* **117**, 704 (1995).
³⁷A. Harriman, F.M. Romero, R. Ziessel, and A.C. Benniston, *J. Phys. Chem. A* **103**, 5399 (1999).
³⁸M. Wohlgenannt, W. Graupner, G. Leising, and Z.V. Vardeny, *Phys. Rev. Lett.* **82**, 3344 (1999).
³⁹W. Holzer, A. Penzkofer, S.H. Gong, D.D.C. Bradley, X. Long, and A. Bleyer, *Chem. Phys.* **224**, 315 (1997).
⁴⁰M. Redecker, D.D.C. Bradley, M. Inbasekaran, and E.P. Woo, *Appl. Phys. Lett.* **73**, 1565 (1998).